

---

Retrospective Theses and Dissertations

---

Spring 1980

## Electromagnetic Wave Scattering from a Rough Surface

Elie G. Nacouzi  
*University of Central Florida*



Part of the [Engineering Commons](#)

Find similar works at: <https://stars.library.ucf.edu/rtd>

University of Central Florida Libraries <http://library.ucf.edu>

This Masters Thesis (Open Access) is brought to you for free and open access by STARS. It has been accepted for inclusion in Retrospective Theses and Dissertations by an authorized administrator of STARS. For more information, please contact [STARS@ucf.edu](mailto:STARS@ucf.edu).

---

### STARS Citation

Nacouzi, Elie G., "Electromagnetic Wave Scattering from a Rough Surface" (1980). *Retrospective Theses and Dissertations*. 505.

<https://stars.library.ucf.edu/rtd/505>



ELECTROMAGNETIC WAVE SCATTERING  
FROM A ROUGH SURFACE

BY

ELIE GEORGE NACOUZI  
M.S., Polytechnic Institute of Kiev, U.S.S.R., 1973

RESEARCH REPORT

Submitted in partial fulfillment of the requirements  
for the degree of Master of Science in the  
Graduate Studies Program of the College of Engineering  
at the University of Central Florida; Orlando, Florida

Spring Quarter  
1980

## ABSTRACT

This was a study to measure surface roughness using scattering of electromagnetic waves in the  $K_a$  and X microwave frequency bands. The detected fluctuations of the reflected field intensity is a measure of surface roughness. The reflected field intensity depends on the wavelength, the angle of incidence and the electrical properties of the media. Since the surface presents irregularities with randomly distributed facets, the characteristics of the rough-surface reflected wave can only be described by the statistical properties of the field intensity. The dependence of the normalized moments of the returned scatter on distance from the rough surface to the receiving antenna was analyzed as a function of surface roughness distribution at two different frequency-bands.

## ACKNOWLEDGMENTS

The author wishes to express appreciation to the people who contributed toward the development of the project and the preparation of this research report.

I would like to thank Mr. Barry Bullard for the valuable suggestions and help he has given me on this project. Next, I would like to thank the chairman of my committee, Dr. Ronald Phillips for his advisement and guidance. I would like also to give a special thanks to the Physics Department and Dr. Oelfke for their cooperation in making equipment available for the project. Finally, I would like to thank Ms. Dian Brandstetter for her help and many hours of typing of this research report.

## TABLE OF CONTENTS

ACKNOWLEDGMENTS . . . . .	iii
LIST OF TABLES . . . . .	v
LIST OF ILLUSTRATIONS . . . . .	vi
Chapter	
I.    SYSTEM DESCRIPTION . . . . .	1
Introduction . . . . .	1
Measurement System . . . . .	2
II.   SURFACE STATISTICS . . . . .	7
Volume Distribution of a Rough Surface . . . . .	7
Height Variations Distribution of the Surface . . . . .	12
Measurement of the Autocorrelation Function of the Surface Heights . . . . .	20
III.  SCATTERED FIELD INTENSITY ANALYSIS . . . . .	24
Experimental Analysis . . . . .	24
Mathematical Analysis . . . . .	29
The Rayleigh Criterion of Roughness . . . . .	32
IV.   CONCLUSIONS AND RECOMMENDATIONS . . . . .	35
Conclusions . . . . .	35
Recommendations . . . . .	36
APPENDIX A . . . . .	38
APPENDIX B . . . . .	41
APPENDIX C . . . . .	43
APPENDIX D . . . . .	44
APPENDIX E . . . . .	46
APPENDIX F . . . . .	47
BIBLIOGRAPHY . . . . .	49

LIST OF TABLES

1.	Surface Volume Distribution . . . . .	8
2.	Data Analysis of the Stones Volume Distribution . . . . .	10
3.	Program Results of the Surface Normalized Moments . . . . .	14
4.	Frequency Distribution of the Surface Heights . . . . .	15
5.	Comparative Values of the Moments . . . . .	19
6.	Normalized Autocorrelation Function of the Surface Heights . . . . .	22
7.	Comparative Values Between Experimentally and Theoretically Determined Normalized Moments . . . . .	27
8.	Surface Roughness Criterion . . . . .	34

## LIST OF ILLUSTRATIONS

1a.	General View of the Derrick with the Microwave Source . . .	3
1b.	Close-up of Microwave Source . . . . .	4
2.	Block-diagram of the Experimental Set-Up . . . . .	6
3.	Cumulative Distribution Function of Stone Volume . . . . .	11
4.	Side View of Comb-Shaped Device . . . . .	13
5.	Experimental Frequency Plot of the Surface Height (Batch #1) . . . . .	16
6.	Experimental Frequency Plot of the Surface Height (Batch #2) . . . . .	17
7.	Experimental Frequency Plot of the Surface Height (Batch #3) . . . . .	18
8.	Normalized Autocorrelation Function of the Surface Heights . . . . .	23
9.	Normalized 2nd Moment as Function of the Antenna Height . . . . .	25
10.	Normalized 2nd Moment as Function of the Antenna Height . . . . .	26
11.	Normalized 2nd Moment as Function of the Antenna Height . . . . .	30
12.	Normalized 3rd, 4th, and 5th Moments of the Scattered Power as Function of the Normalized 2nd Moment . . . . .	31
13.	Rayleigh Criterion . . . . .	32
14.	Phase Difference Between Center and Edge of Illuminated Surface . . . . .	47

## CHAPTER I

### SYSTEM DESCRIPTION

#### Introduction

When an electromagnetic wave is incident on a plane interface between two media, it is reflected by well-known laws: the reflected field depends on the wavelength, the angle of incidence and the electrical properties of the two adjoining media. What happens, however, if the boundary is not planar but irregular or simply rough?

Perhaps the most striking difference in the behavior of a smooth and a rough surface is the fact that a smooth plane reflects the incident wave specularly in a single direction, while a rough surface scatters it into various directions, though certain privileged directions may receive more energy than others. According to this definition, the same surface may be rough for some wavelengths and smooth for others; or for the same wavelength it may be either rough or smooth for different angles of incidence.

The surface to be analyzed was neither periodic nor explicitly given and was described by its statistical properties. In the following, it is assumed that the statistical model of the surface is generated by a continuous stationary homogeneous two-dimensional random process. The distribution of the height differentials is found using method of matching moments. However, the statistical



distribution of the surface heights does not describe the surface completely; it does not tell whether the hills and valleys of the surface are crowded close together or whether they are far apart. A second function, the autocorrelation function of the height of the surface describes this aspect and it can be shown that for a slightly rough surface, the autocorrelation function of the height is sufficient to determine completely the distribution of coherently reflected and scattered radiation (Davies, 1954).

It is furthermore assumed that the surface is a perfect conductor and that the surface currents are of the same magnitude as those set up in a plane reflector, but with the phase of the currents at a point varying in a random manner connected with the heights of the surface.

The utilization of  $K_a$ -band and X-band sources develops the versatility of analyzing the reflection and scattering characteristics of a rough and semi-rough surface respectively.

#### Measurement System

The system described as follows represents the derived technique for the measurement of returned electromagnetic wave scatter from a rough surface. The system consists of an X-band transmitter, K-band transmitter and movable derrick (platform) as shown in Figure 1. The measurement of the returned scatter is achieved by utilization of a directional coupler which is sensitive to return signal only, and a microwave square-law crystal detector.


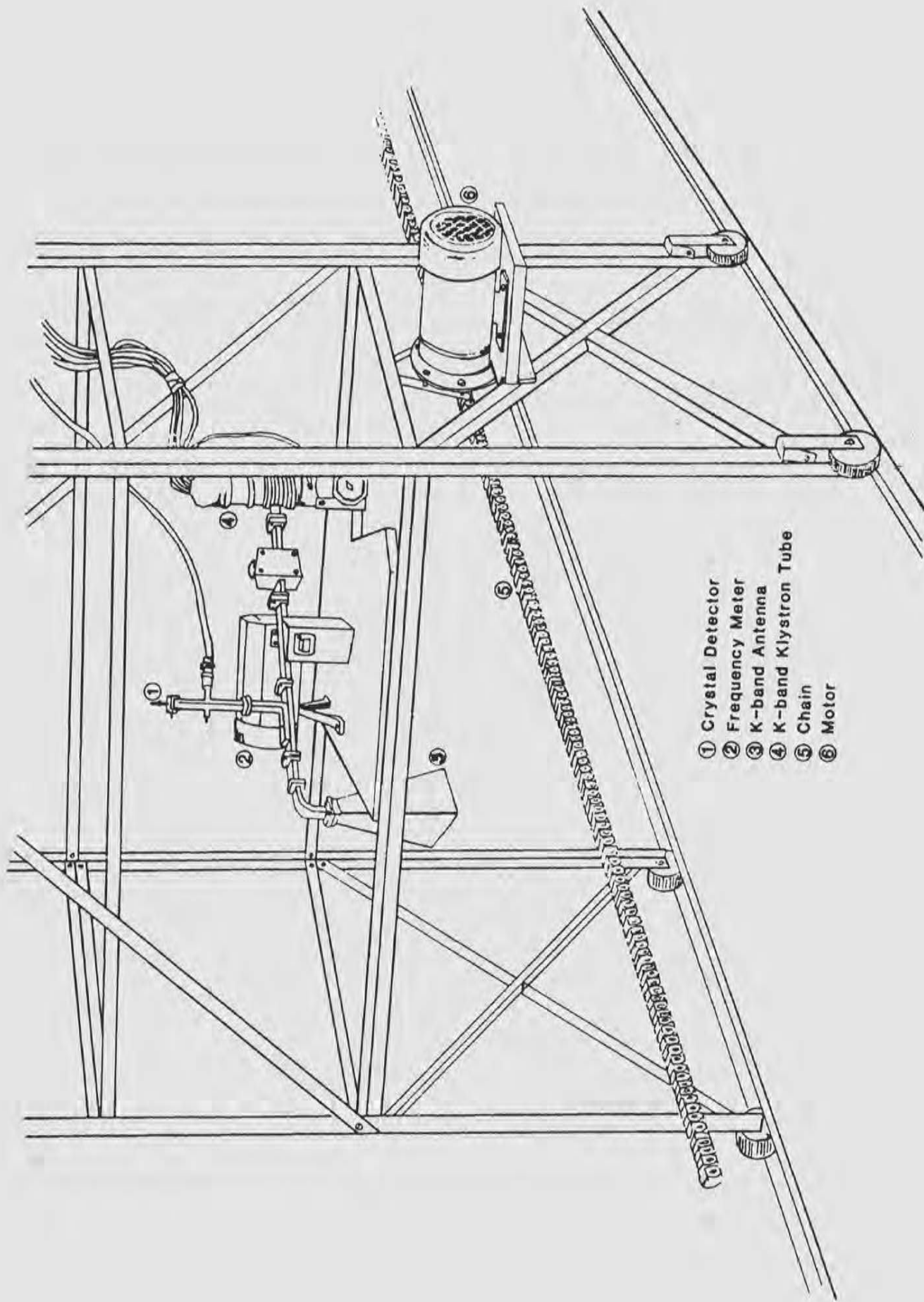
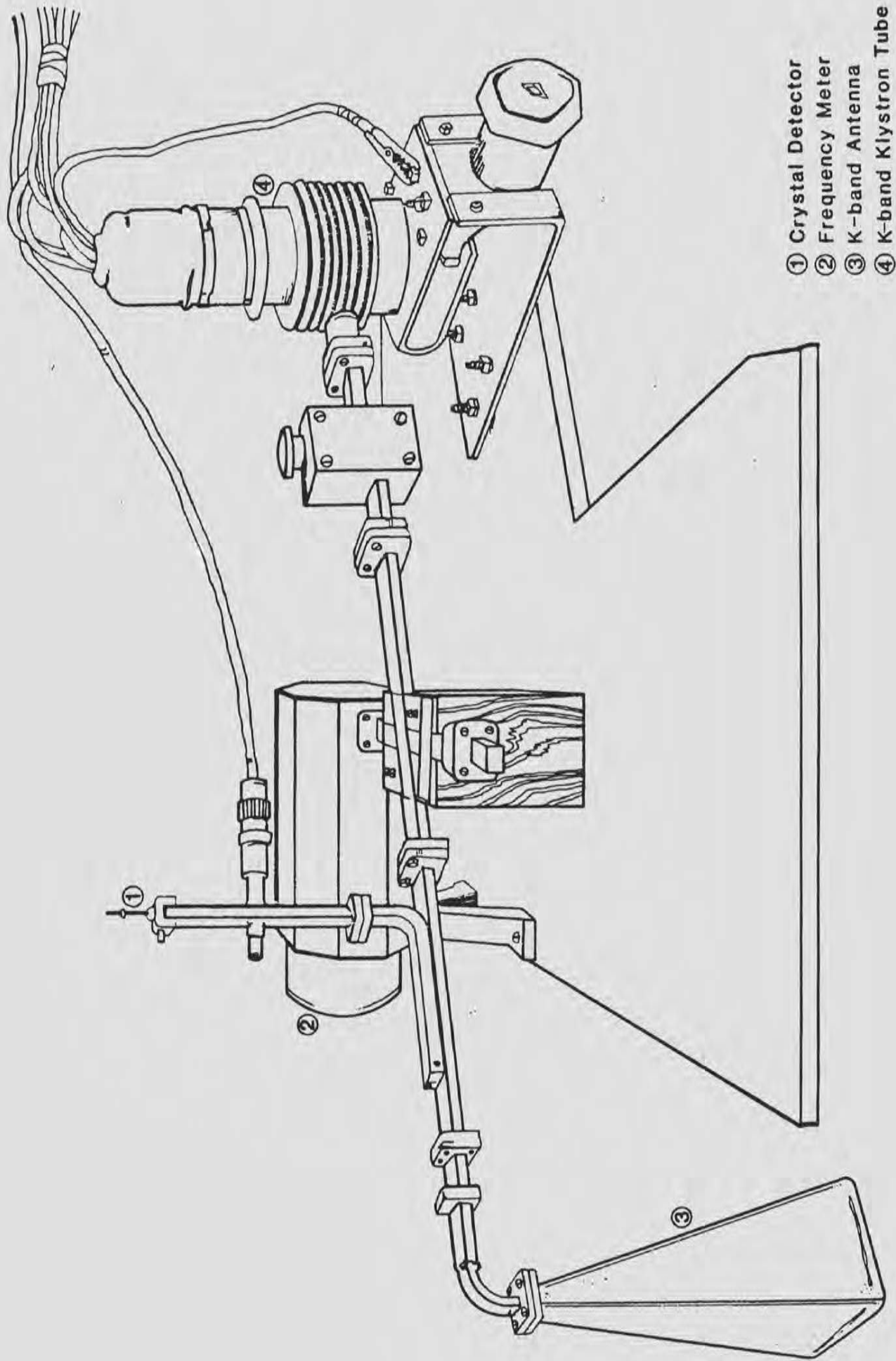


Fig. 1a. General view of the derrick with the microwave source



- ① Crystal Detector
- ② Frequency Meter
- ③ K-band Antenna
- ④ K-band Klystron Tube
- ⑤ Chain
- ⑥ Motor

Fig. 1b. Close-up of microwave source



- ① Crystal Detector
- ② Frequency Meter
- ③ K-band Antenna
- ④ K-band Klystron Tube

The first moment of the returned scatter was measured by the utilization of an ordinary DC voltmeter (HP-410C). The second moment was measured with a TSI model 1060 which is a "true" root mean square meter. The model 1060 and similar meters that basically measure what is indicated by the following equation:

$$\left[ \lim_{T \rightarrow \infty} \frac{1}{T} \int_{-\frac{T}{2}}^{\frac{T}{2}} (f(t) - \overline{f(t)})^2 dt \right]^{1/2} \quad (1)$$

are "true".

The implication is that some meters are not "true". These latter units are essentially rectifier units that give an accurate root mean square reading only on a sine wave input. A "true" rms meter gives an accurate reading independent of the wave shape of the input signal.

A measurement sequence for a fixed transmit frequency consists of several derrick runs at constant speed while simultaneously recording the first and second moment of the returned field intensity. Normalization of the second moment with respect to the mean value was necessary to account for uncontrollable total power density fluctuations.

The above sequence is repeated for several heights variation between the transmit antenna and the rough surface. A block-diagram of the experimental set-up is shown in Figure 2.

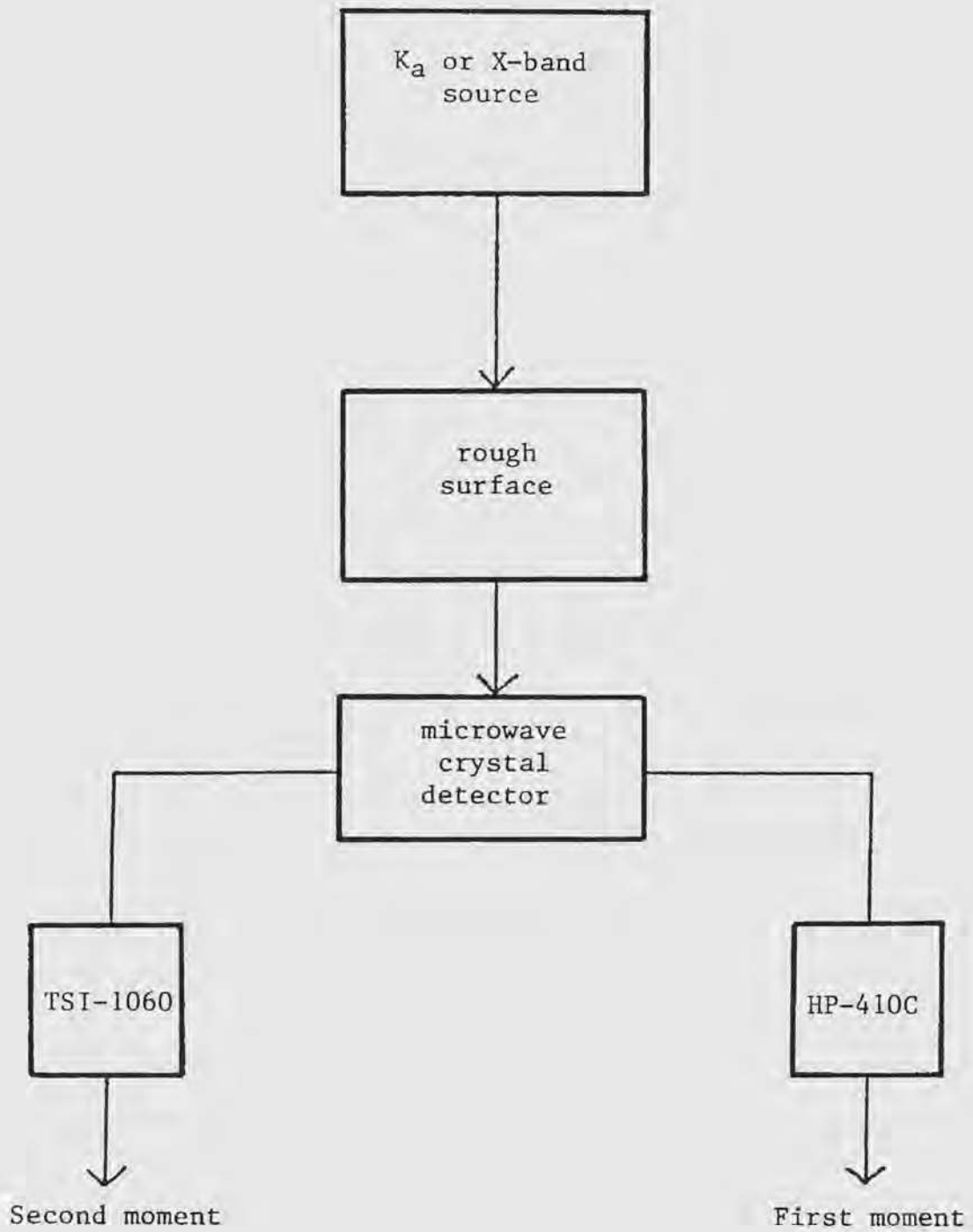


Fig. 2. Block-diagram of the experimental set-up

## CHAPTER II

### SURFACE STATISTICS

#### Volume Distribution of a Rough Surface

The given surface consisted of ballast stones horizontally levelled in a rectangular shape mold 12 feet x 4 feet. The selection of the stone samples was determined by a sifting system for which stone sizes were between  $3/4$  inch and  $1/2$  inch.

A random sample of one hundred stones was selected from the surface for volume measurement. Individual stone volume was determined by dropping the stone into a graduated tube of water. Displacement of the water determines the volume of the stone. From the total sample population, the task was to determine the empirical cumulative distribution of the random variable (volume) giving rise to the data. The volume grouping of the randomly selected stones was set by the resolution of the graduated tube which is a  $1/2$  ml.

Once the volume cells were determined, the corresponding frequency rate for each cell was taken. For the above frequency and volume sets, the cumulative distribution function was calculated. Table 1 lists the results of the surface's stone volume distribution.

The moment calculations of the stone volume distribution was determined by computer analysis. The analysis of the moments



TABLE 1  
SURFACE VOLUME DISTRIBUTION

Volume ml	1	1.5	2	2.5	3	3.5	4	Sample size
Frequency	7	13	31	14	21	7	7	100
Normalized frequency	0.07	0.13	0.31	0.14	0.21	0.07	0.07	
Cumulative probability %	7	20	51	65	86	93	100	

(Skewness and Kurtosis) suggested Gaussian distribution of the surface volume. This is reflected by program results of the Skewness value  $S = 0.27345$  where

$$S \triangleq \frac{m_3}{\frac{3}{2} m_2} \quad (2)$$

for which a value of  $-0.5 < S < 0.5$  closely approximates a Gaussian distribution ( $m_i$  is the  $i$ th central moment).

The Kurtosis value  $K = 2.385$  where

$$K \triangleq \frac{m_4}{\frac{3}{2} m_2^2} \quad (3)$$

indicates a slightly flattened Gaussian distribution since a Kurtosis value  $K < 3$  represents a peak distribution less than the standard Gaussian distribution peak. Table 2 lists the results of the Skewness-Kurtosis analysis.

Since Gaussian distribution seems likely for the surface volume due to program results, a cumulative frequency graph on probability paper was generated (Figure 3). The straight line on the graph indicates that the distribution is normal.

TABLE 2

DATA ANALYSIS OF THE STONE VOLUME DISTRIBUTION.  
LISTED MOMENTS ARE CENTRAL MOMENTS.

---

---

2.39	Mean
2.250853294	Arithmetic Mean
2.104524728	Geometric Mean

---

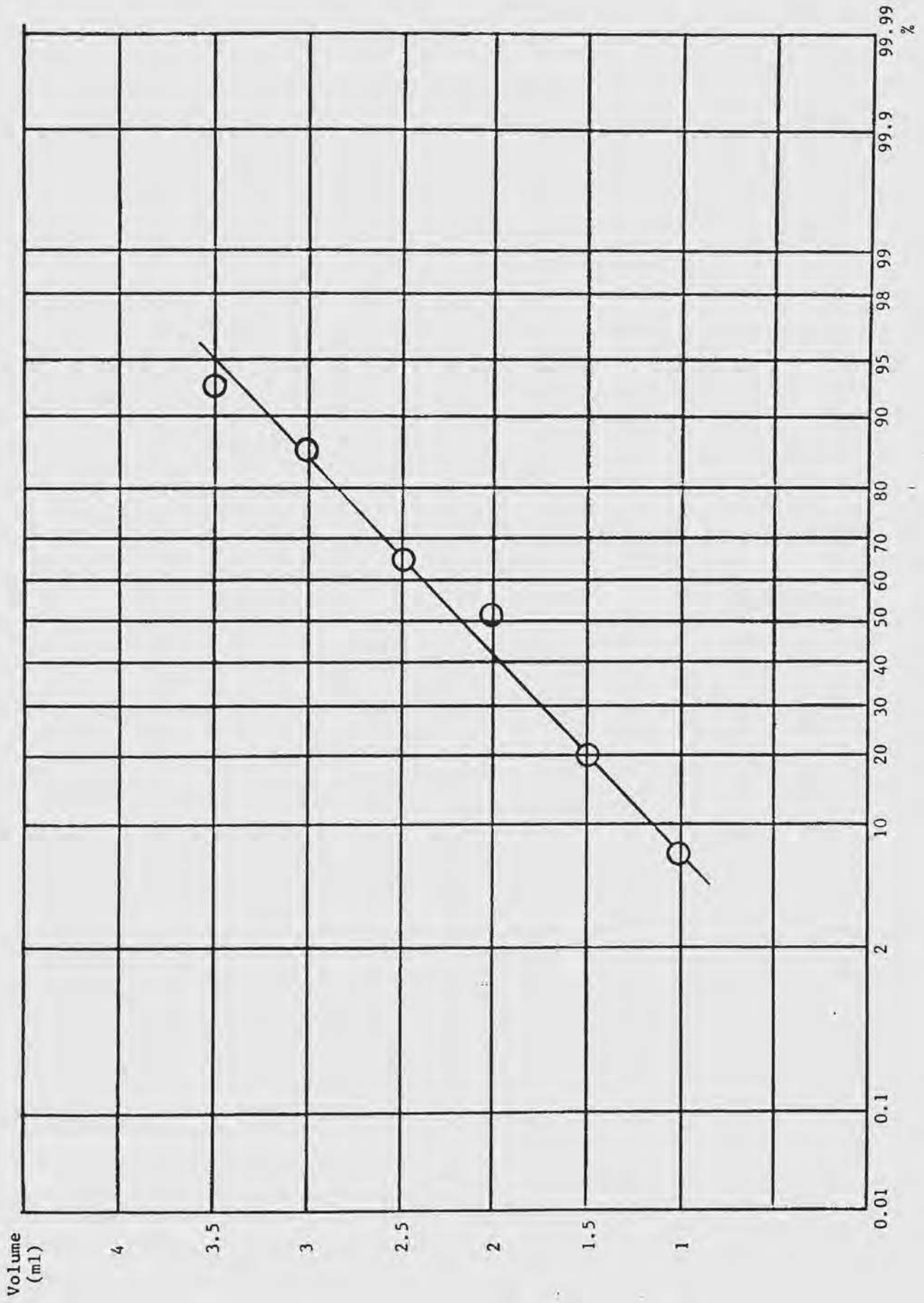
0.6329	Second Moment
0.137688	Third Moment
0.95573777	Fourth Moment

---

2.385989664	Kurtosis
.2734597725	Skewness

---

Fig. 3. Cumulative distribution function of stone volume



### Height Variation Distribution of the Surface

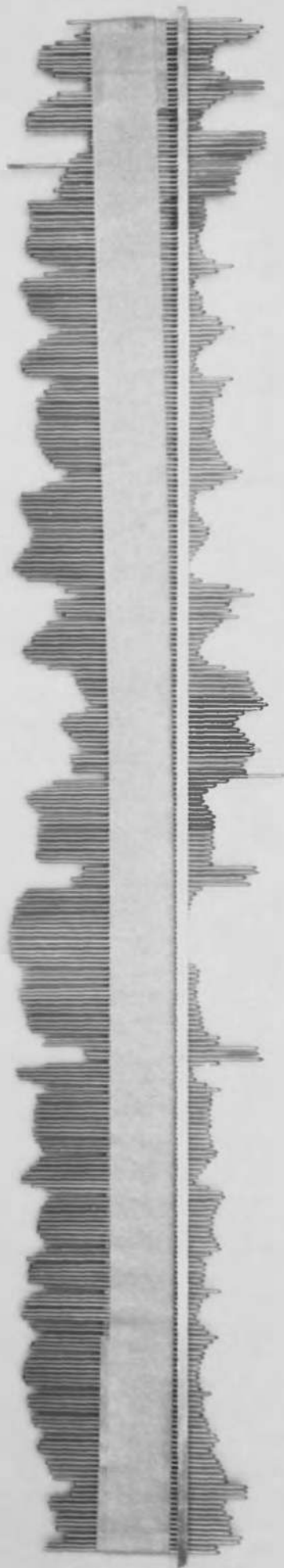
In order to determine the surface height statistics, a special device as shown in Figure 4 was fabricated.

The device is an aluminum bar 18 inch x 1 inch x 1/8 inch with 299 equally spaced .045 inch holes along its longitudinal axis. The distance between two consecutive holes is .060 inch and is chosen as small as possible to determine a relatively accurate plot of the autocorrelation function of the surface height. A 2 inch x .040 inch stainless welding rod, with one side ground to a point, was placed in each hole.

The measurement of the surface height differentials was accomplished by placing the device horizontally on the surface with the pins flush to the bottom surface of the comb-shaped device, and then removing the pins restraints (masking tape) to allow the pins to fall into the peaks and the valleys of the surface. The pins were again restrained, the device removed, and the height differentials were measured. The procedure was repeated at three different random positions on the surface with a measurement from each of the x and y-axes of the surface.

The measurement of the height differentials were collected into batches of 600 data points (300 from the x-axis and 300 from the y-axis) and processed by the MINC-11 Digital Equipment Corporation computer, using the program listed in Appendix B. The program is designed to compute the first five moments of the surface height distribution and their respective normalized values. The program

Fig. 4. Side view of comb-shaped device





results are listed in Table 3.

TABLE 3  
PROGRAM RESULTS OF THE SURFACE NORMALIZED MOMENTS

	mean $I_1$ (mm)	$N_2$	$N_3$	$N_4$	$N_5$
Batch 1	11.5151	1.30015	2.04055	3.68292	7.35837
Batch 2	12.1156	1.31446	2.09525	3.85646	7.89686
Batch 3	10.1137	1.41408	2.48731	5.04788	11.2541

It was advantageous to plot the frequency distribution of the heights versus the heights themselves in order to determine a most probable hypothesis describing the density function. Table 4 contains the data and Figures 5, 6, and 7 are the corresponding plots.

TABLE 4

FREQUENCY DISTRIBUTION OF THE SURFACE HEIGHTS  
CORRESPONDING TO THREE RANDOM SAMPLES OF  
APPROXIMATELY 600 DATA POINTS EACH

Heights (mm)	Frequency			Heights (mm)	Frequency			Heights (mm)	Frequency		
	Batch 1	Batch 2	Batch 3		Batch 1	Batch 2	Batch 3		Batch 1	Batch 2	Batch 3
0	1	2	5	12	56	36	32	24	8	6	3
1	8	16	21	13	28	18	24	25	7	5	8
2	10	--	21	14	18	16	23	26	4	3	4
3	25	14	32	15	38	37	18	27	6	6	2
4	24	25	28	16	23	15	13	28	7	4	2
5	27	28	49	17	16	25	11	29	2	4	10
6	36	28	50	18	15	26	13	30	4	--	1
7	36	41	42	19	10	14	10	31	--	3	--
8	46	41	43	20	9	16	12	32	1	--	--
9	43	38	41	21	3	12	7	33	--	2	--
10	43	56	33	22	8	11	9	34	--	7	--
11	29	34	25	23	6	3	6	35	1	--	--

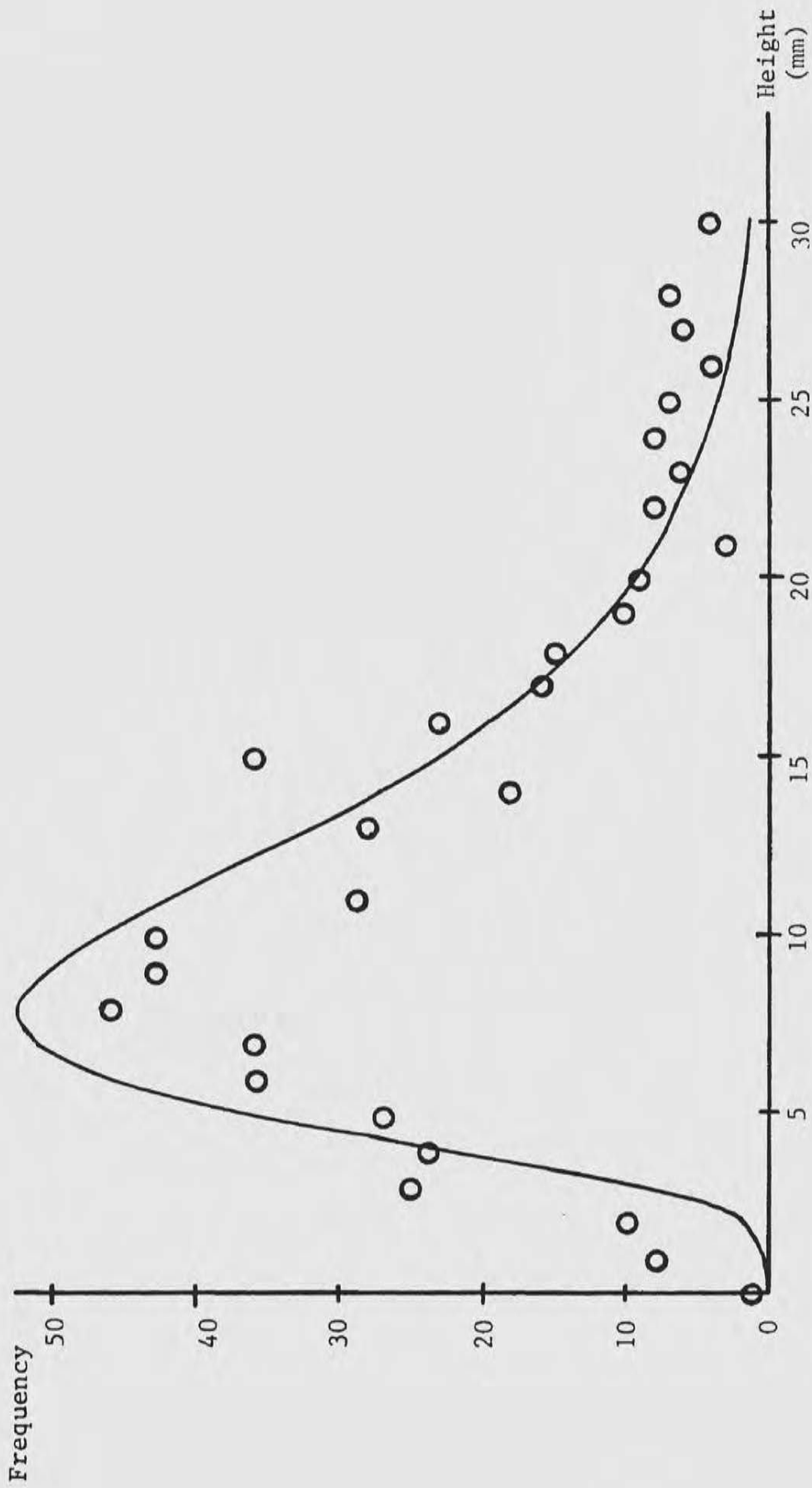


Fig. 5. Experimental frequency plot of the surface heights (Batch #1).  
 A log-normal curve with  $\mu = 2.31242$  and  $\sigma^2 = 0.26248$  is fitted.

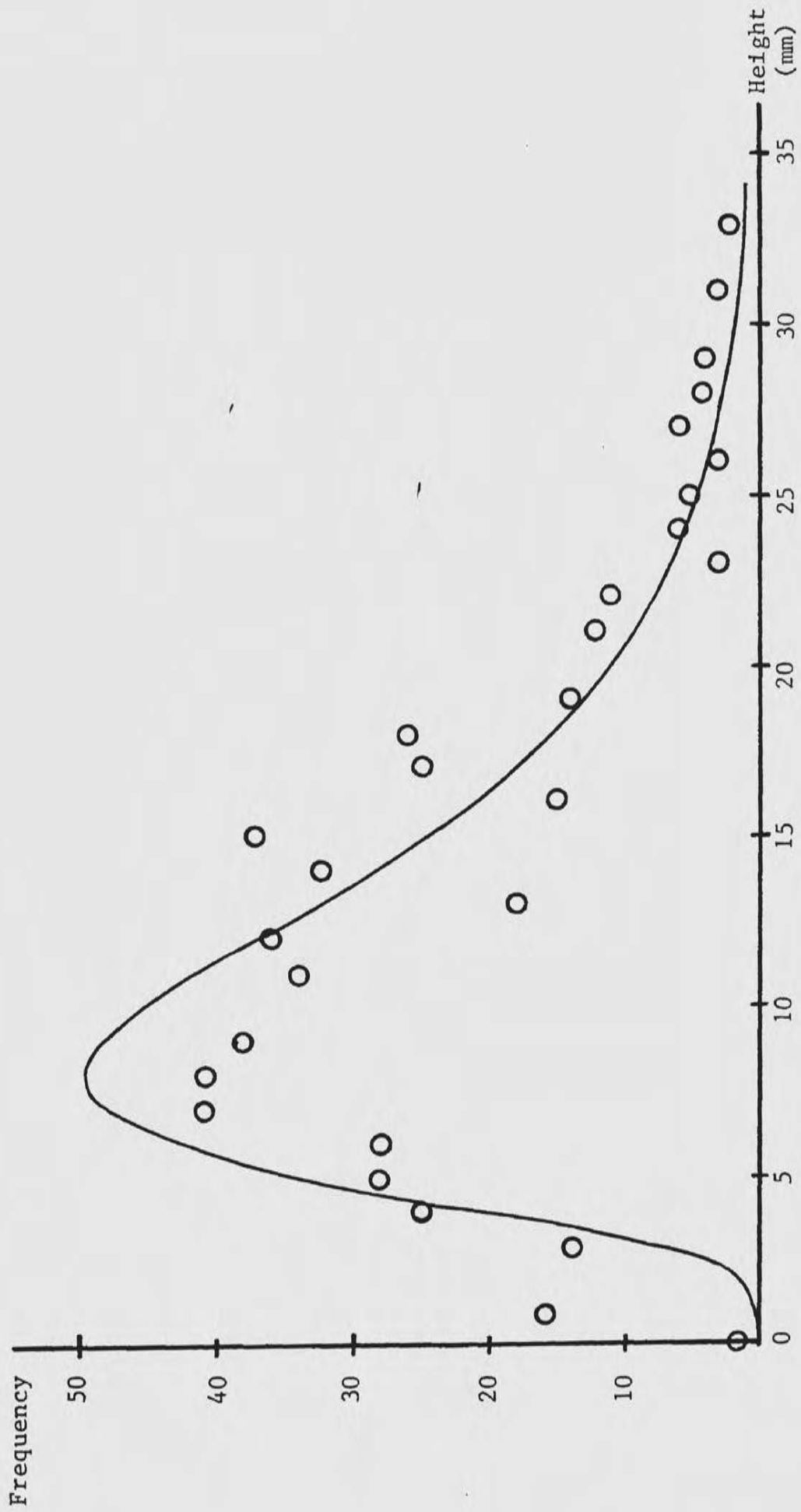


Fig. 6. Experimental frequency plot of surface heights (Batch #2).  
 A log-normal curve with  $\mu = 2.35778$  and  $\sigma^2 = 0.273426$  is fitted.

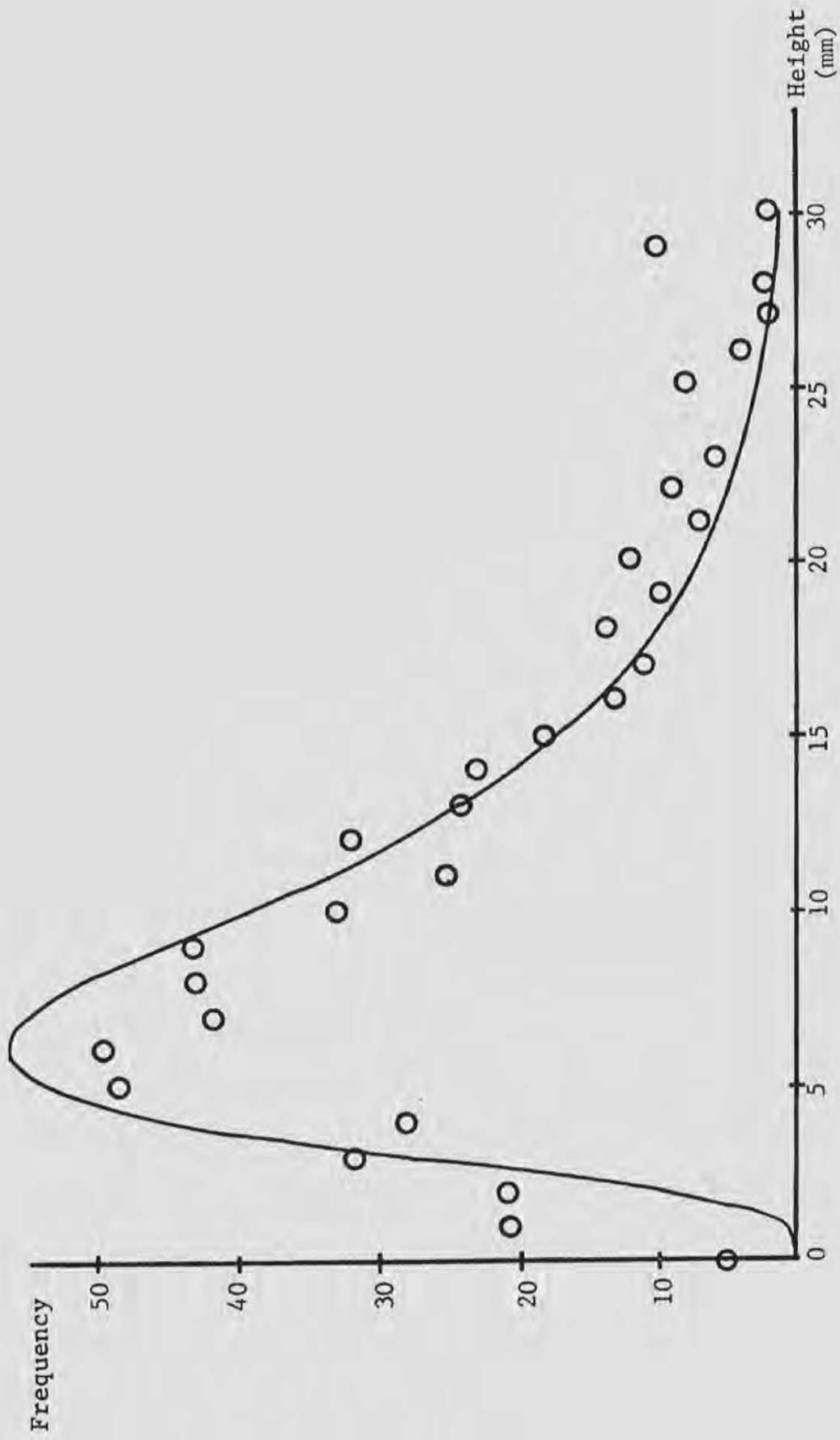


Fig. 7. Experimental frequency plot of the surface heights (Batch #3).  
 A log-normal curve with  $\mu = 2.14065$  and  $\sigma^2 = 0.34648$  is fitted.

After visual analysis of Figures 5, 6, and 7, some distributions were analyzed (Log-normal, Rice and K). The data supports the most probable hypothesis of the surface being log-normal.

Therefore, mathematical analysis of the normalized 3rd, 4th, and 5th moment was done to determine the hypothesis. From Appendix A, the Kth normalized moment  $N_K$  of a log-normal distribution can be expressed as:

$$N_K = N_2^{K(K-1)/2} \quad (4)$$

where  $N_2$  is the normalized second moment.

Table 5 shows comparative values between the experimentally measured normalized moments of the surface and the corresponding theoretically determined moments of the log-normal distribution.

TABLE 5

COMPARATIVE VALUES OF THE MOMENTS WHERE  $I_1$  IS THE FIRST MOMENT

	Batch 1	Log-Normal	Batch 2	Log-Normal	Batch 3	Log-Normal
$I_1$ (mm)	11.5151	11.5151	12.1156	12.1156	10.1137	10.1137
$N_2$	1.30015	1.30015	1.31446	1.31446	1.41408	1.41408
$N_3$	2.04055	2.19776	2.09525	2.27113	2.48731	2.82763
$N_4$	3.68292	4.83015	3.85646	5.15803	5.04788	7.99546
$N_5$	7.35837	13.80176	7.89686	15.39833	11.2541	31.96979

It should be noted that there is a large difference between the 5th moment of the log-normal distribution and the corresponding experimentally determined moment. This is due to the fact that at least 5,000 sample points are necessary to get an accurate experimental 5th moment.

Measurement of the Autocorrelation  
Function of the Surface Heights

Since the autocorrelation function  $R(\rho)$  plays an important role in the analysis of the surface roughness, an important practical problem is that of determining it for experimentally observed random process. The only available procedure is to calculate an estimated autocorrelation function denoted by  $\hat{R}(\rho)$  over a finite distance on the surface under the assumption that the process is stationary.

It is then possible to define  $\hat{R}(\rho)$  as

$$\hat{R}_h(\rho) = \frac{1}{L-\rho} \int_0^{L-\rho} h(x) h(x+\rho) dx, \quad 0 \leq \rho \leq L \quad (5)$$

over the ensemble of sample functions. This estimate is a random variable denoted by  $\hat{R}_H(\rho)$ . Note that the averaging distance is  $L-\rho$  rather than  $L$  because this is the only portion of the observed data in which both  $h(x)$  and  $h(x+\rho)$  are available.

The above integral representation of  $\hat{R}_H(\rho)$  cannot be evaluated because a mathematical expression for  $h(x)$  is not available. An alternative procedure is to approximate the integral by sampling the continuous function at discrete distances using the comb-shaped



device shown in Figure 4 and performing the discrete equivalent to  $\hat{R}_h(\rho)$ . Thus, if the samples of a particular sample function are taken at intervals of  $0, \Delta x, 2\Delta x, \dots, N\Delta x$ , and if the corresponding values of  $h(x)$  are  $h_0, h_1, h_2, \dots, h_N$  the discrete equivalent to the integral representation of  $R_h(\rho)$  is:

$$\hat{R}_h(n\Delta x) = \frac{1}{N-n+1} \sum_{K=0}^{N-n} h_K h_{K+n} \quad (6)$$

$n = 0, 1, 2, \dots, M$   
 $M \ll N$

This estimate is also a random variable over the ensemble and, as such, is denoted by  $\hat{R}(n\Delta x)$ . Since  $N$  is quite large (300 data points), this operation was performed by the digital equipment MINC-11, using the programs listed in Appendices B and C. Table 6 contains the program's results and Figure 8 is the corresponding data plot.

A curve fit was performed for 15 experimental data points. This resulted in the following analytical expression:

$$R(\rho) = 0.232 \exp(-0.23|\rho|) + 0.768 \quad (7)$$



TABLE 6  
 NORMALIZED AUTOCORRELATION FUNCTION  
 OF THE SURFACE HEIGHTS

n	R(nΔx) (normalized)	n	R(nΔx) (normalized)
0	1	13	0.75312
1	0.9528	14	0.7588
2	0.9144	15	0.7598
3	0.8814	16	0.7692
4	0.8579	17	0.77544
5	0.83634	18	0.7787
6	0.8197	19	0.77193
7	0.8053	20	0.7618
8	0.7899	21	0.7531
9	0.7698	22	0.7423
10	0.7589	23	0.7559
11	0.7541	24	0.768
12	0.7540		

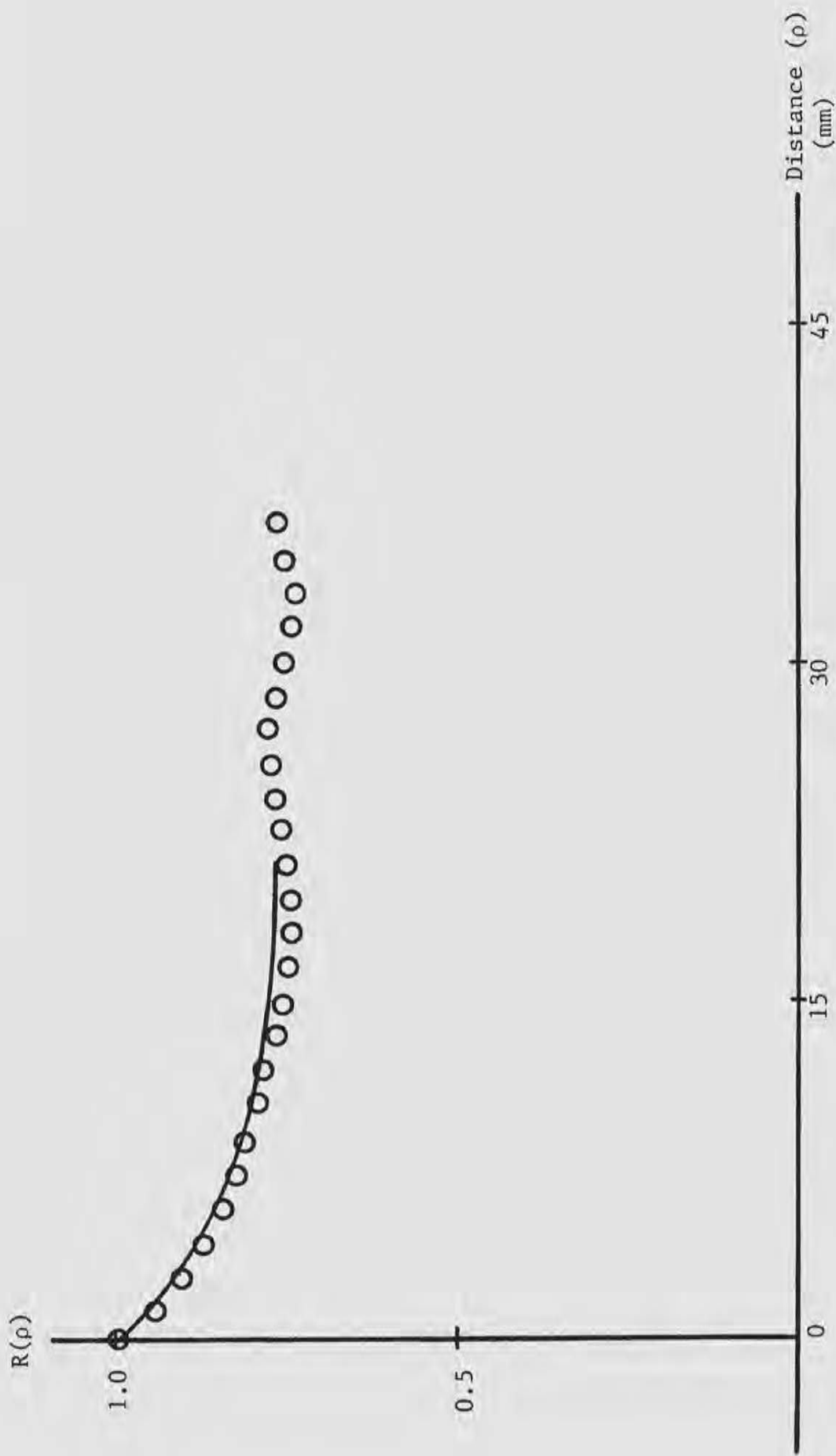


Fig. 8. Normalized Autocorrelation function of the surface heights  
where  $R(0) = 150.538$  square millimeter

## CHAPTER III

### SCATTERED FIELD INTENSITY ANALYSIS

#### Experimental Analysis

The scattered field intensity data was recorded utilizing two techniques. The first technique as described earlier using the DC voltmeter and the true rms meter consisted of visual recording of the first and second moments of the returned scatter field intensity. K-band results of the normalized second moment as a function of heights are illustrated in Figure 9 and X-band results in Figure 10.

It should be noted that the recorded values of the second moment represents only a coefficient proportional to the real value of the measured second moment. This is a characteristic of the true rms voltmeter.

The second technique consisted of analyzing returned electromagnetic scatter on a digital computer, MINC-11. A series of data sets utilizing the same formats as described in the system measurement layout was performed.

The results of the computer-aided analysis of the moments (1st through 5th) and their normalized values at K-band are listed in Table 7. A plot of the normalized 2nd moment as a function of

$N_2 \cdot 10^{-2}$   
Normalized  
2nd moment

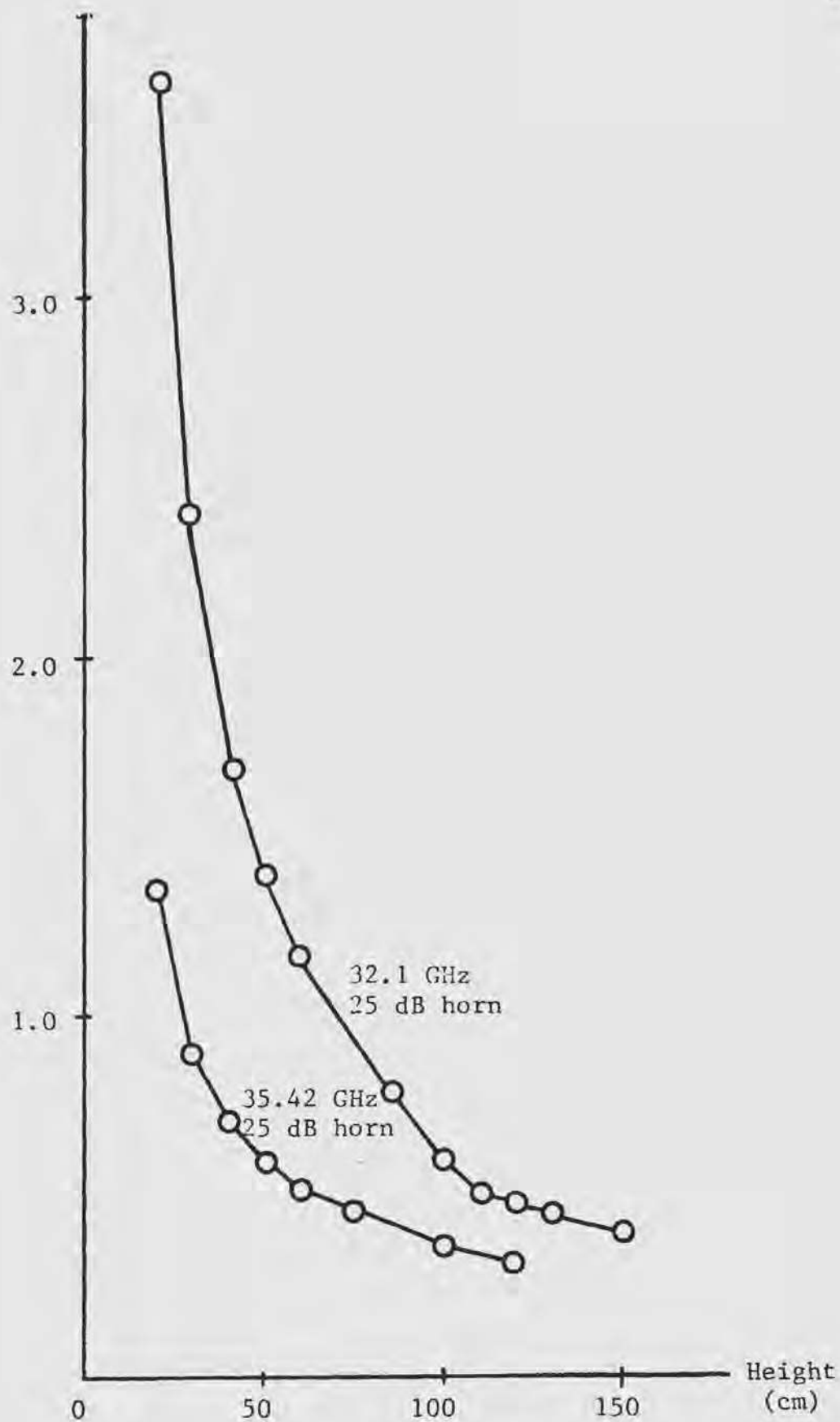


Fig. 9. Normalized 2nd moment as function of the antenna height. 1st and 2nd moments recorded using respectively DC and true rms voltmeter.

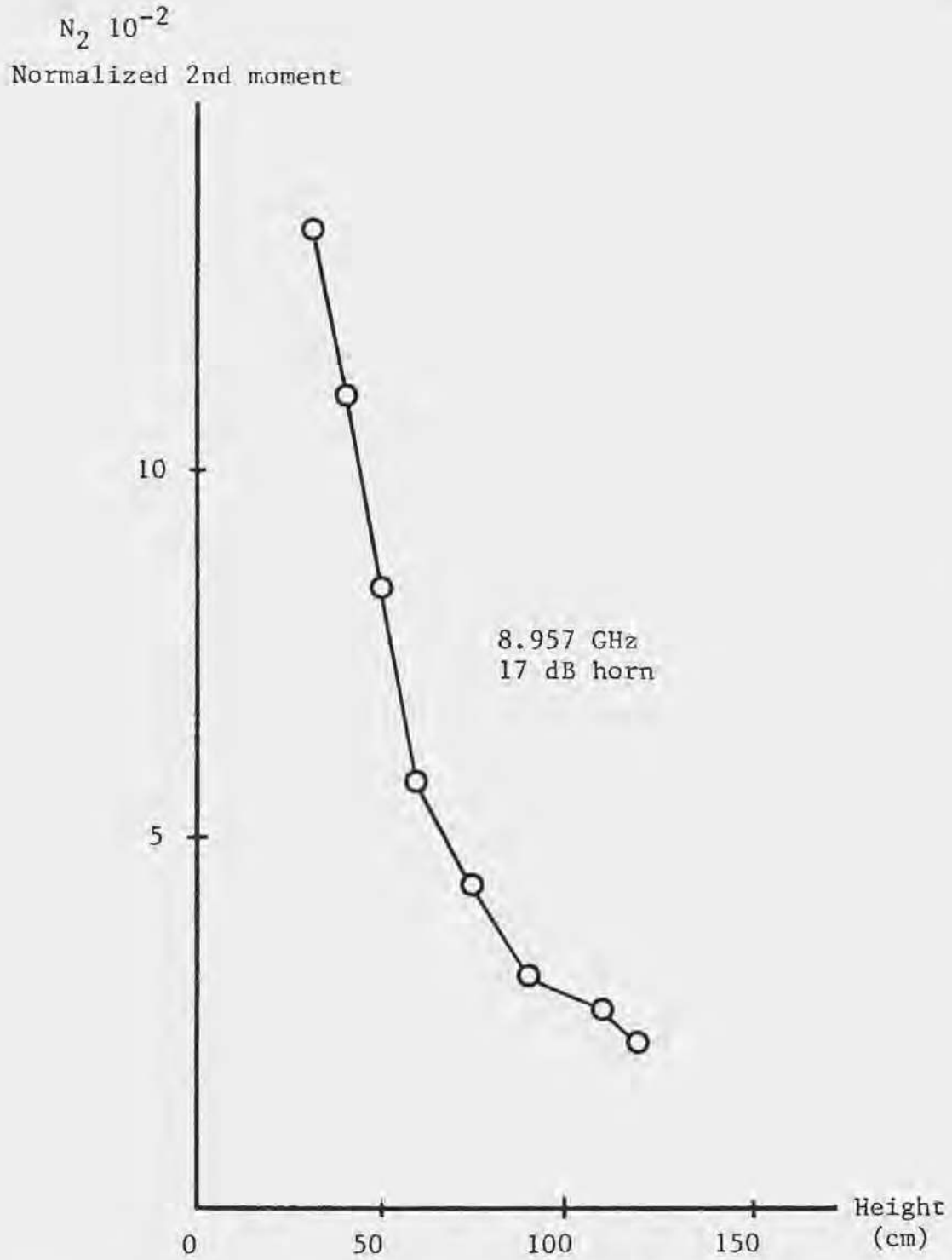


Fig. 10. Normalized 2nd moment as function of the antenna height. 1st and 2nd moments recorded using respectively DC and rms voltmeter.

TABLE 7

COMPARATIVE VALUES BETWEEN EXPERIMENTALLY  
AND THEORETICALLY DETERMINED NORMALIZED  
MOMENTS IN THE K-BAND

heights normalized moments	heights (cm)										
	20	30	40	50	60	75	85	100			
N <sub>2</sub>	experiment	1.01247	1.0078	1.00561	1.00388	1.00343	1.00197	1.00167	1.00144		
N <sub>3</sub>	experiment	1.0376	1.02371	1.01687	1.01187	1.01049	1.00606	1.00521	1.00432		
	log-normal	1.0379	1.0236	1.01692	1.01168	1.01033	1.00592	1.00502	1.00433		
N <sub>4</sub>	experiment	1.07601	1.04806	1.03393	1.02403	1.02119	1.01228	1.01065	1.00866		
	log-normal	1.0772	1.04772	1.03413	1.02076	1.01188	1.01006	1.00867	1.00529		
N <sub>5</sub>	experiment	1.12882	1.0814	1.05702	1.04049	1.0356	1.02063	1.01799	1.01446		
	log-normal	1.13194	1.0808	1.05753	1.03948	1.03483	1.01988	1.01683	1.01449		

TABLE 7--Continued

heights (cm)	normalized moments									
	110	120	130	140	150	160	170			
N <sub>2</sub> experiment	1.00088	1.00062	1.00052	1.00044	1.00041	1.00035	1.0003			
	1.00283	1.00203	1.00174	1.00152	1.00142	1.00124	1.00111			
N <sub>3</sub> log-normal	1.00264	1.00186	1.00156	1.00132	1.00123	1.00105	1.00090			
	1.00585	1.00424	1.00366	1.00322	1.00304	1.00267	1.00242			
N <sub>4</sub> log-normal	1.00529	1.00373	1.00312	1.00264	1.00246	1.00210	1.00180			
	1.00998	1.00724	1.00663	1.00558	1.00527	1.00465	1.00424			
N <sub>5</sub> log-normal	1.00883	1.00622	1.00521	1.00441	1.00411	1.00351	1.00300			

heights, from the computer-aided data, is illustrated in Figure 11.

Analysis of the normalized 2nd moment as a function of heights by the two methods described above, indicates a decaying characteristic of the normalized second moment as the heights increase. Although the decaying characteristic remains constant for all data sets, higher normalized second moments occur as the frequencies decrease. This is most predominant when comparing the relation amplitude of K-band and X-band normalized second moment values.

#### Mathematical Analysis

In reviewing the experimentally recorded moments, some distributions were analyzed to determine the statistical characteristics of the returned scatter. From the results it was concluded that a most probable distribution was log-normal. Therefore, by using Appendix A, the corresponding normalized 3rd, 4th, and 5th moments were determined and compared with the experimentally recorded moments. (See Table 7).

The above conclusion is further verified by the plotting of the 3rd, 4th, and 5th normalized moments versus the normalized second moment for the experimental and theoretical data points. Figure 12 represents the corresponding plot for the data sets. It should be noted that due to graph resolution, a single line represents both, theoretical and experimental data points.



$(N_2 - 1)10^3$  \*  
Normalized 2nd moment

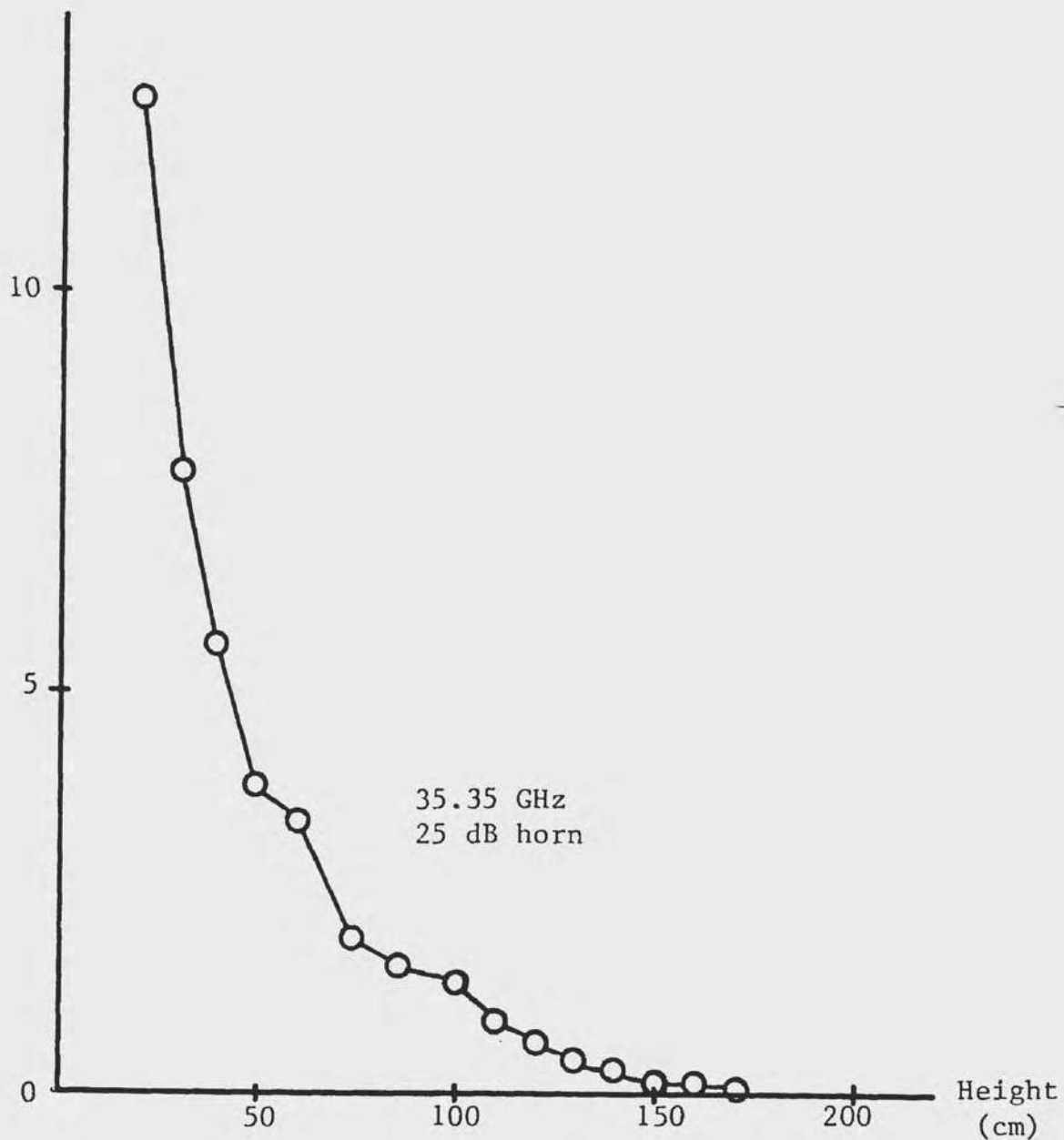


Fig. 11. Normalized 2nd moment as function of the antenna height. 1st and 2nd moments recorded using MINC-11.

\*It should be noted that the normalized second moment recorded via computer analysis represents the absolute value of the normalized second moment. Whereas, the TSI-1060 data represents only a coefficient of the absolute value of the second moment.

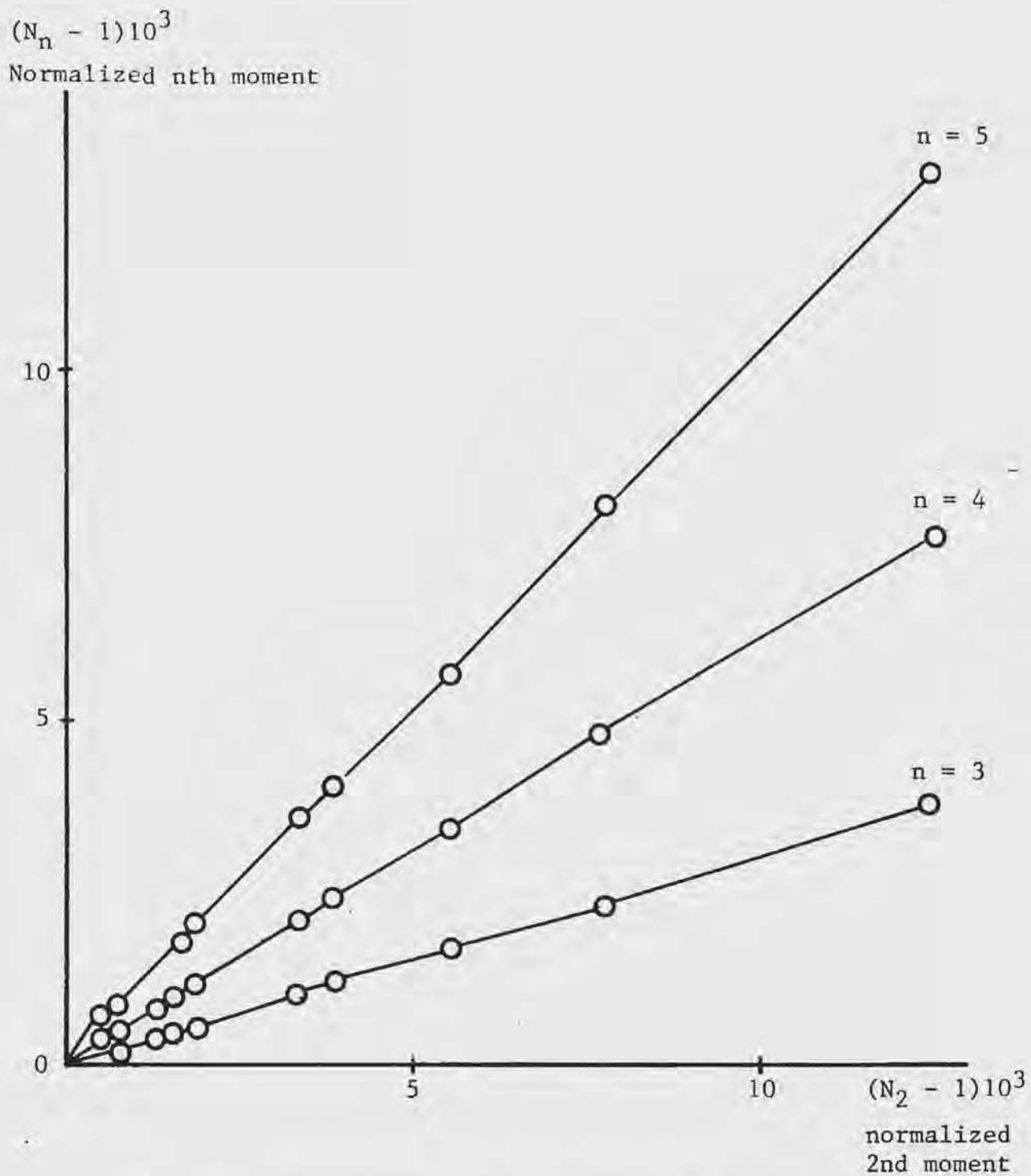


Fig. 12. Normalized 3rd, 4th, and 5th moments of the scattered power as function of the normalized 2nd moment.

### The Rayleigh Criterion of Roughness

Whether the surface is rough or smooth depends on the wavelength, the surface roughness, and the angle of incidence. A surface is considered smooth when specular reflection from the surface occurs. However, when this specular reflection changes into diffuse scattering, the surface is considered rough.

Rayleigh suggested a relationship involving wavelength, surface roughness, and angle of incidence to determine surface characteristics (smooth or rough). This is known as Rayleigh criterion and is shown in Figure 13.

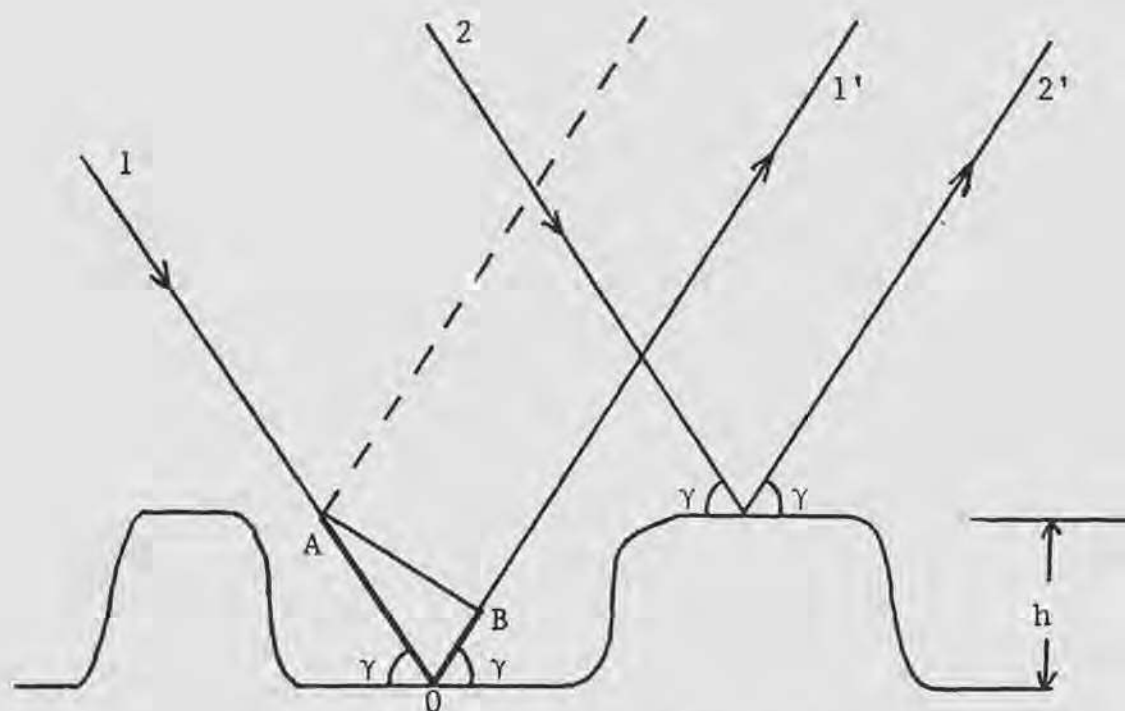


Fig. 13. Rayleigh Criterion

Consider rays 1 and 2 (Figure 13) incident on a surface with irregularities of height  $h$  at a grazing angle  $\gamma$ . The path difference  $\Delta r$  between the two rays is:

$$\begin{aligned}
\Delta r &= AO + OB \\
&= \frac{h}{\sin \gamma} + \frac{h}{\sin \gamma} \cos(\pi - 2\gamma) \\
&= \frac{h}{\sin \gamma} (1 - \cos 2\gamma) = 2h \sin \gamma
\end{aligned} \tag{8}$$

Therefore, the phase difference is:

$$\Delta\phi = \frac{2\pi}{\gamma} \Delta r = \frac{4\pi h}{\gamma} \sin \gamma \tag{9}$$

If  $\Delta\phi$  is small, the two rays will be almost in phase and they are in the case of a perfectly smooth surface. If  $\Delta\phi$  increase, the two rays will interfere until for  $\Delta\phi = \pi$  at which point they will be in phase opposition and cancel. Thus the surface scatters and therefore is rough. By arbitrarily choosing the value half-way between the two cases, i.e.  $\Delta\phi = \frac{\pi}{2}$ , Rayleigh criterion suggests that a surface is considered smooth if:

$$\Delta h < \frac{\lambda}{8\sin \gamma} \quad \text{where} \tag{10}$$

$\Delta h$  - is the standard deviation of the surface heights

$\lambda$  - is the wavelength

$\gamma$  - is the grazing angle ( $\frac{\pi}{2}$ )

Utilizing the data in chapter one to find the standard deviation, surface classification is determined at K-band and X-band frequencies by referring to Table 8.

Rayleigh criterion calculations for the two bands of interest, indicate a rough surface at K-band and semi-rough surface at X-band.

TABLE 8  
SURFACE ROUGHNESS CRITERION

	K-band 35 - 36 GHz	X-band 8.957 GHz
$\overline{\Delta h}$ (mm)	6.54	6.54
$\overline{\lambda}$ (mm)	8.45	33.49
$\frac{\lambda}{8}$ (mm)	1.056	4.19
Rayleigh criterion	rough surface	semi-rough

## CHAPTER IV

### CONCLUSIONS AND RECOMMENDATIONS

#### Conclusions

The efforts generated through this research project resulted in the feasibility of generating a randomly distributed surface which has predictable distribution. Initial efforts to determine heights distribution through volume analysis of the stones did not prove to be related since the volume was normal and the height variations log-normal. This required the construction of a comb-shaped device as shown in Figure 4 which proved to be successful in determining the height statistics. Analysis of the surface based on this device proved that the height differentials were log-normally distributed.

Investigation of the returned scatter field intensity from the rough surface resulted in three significant conclusions. First, it was determined that the normalized second moment of the returned field intensity decays as a function of distance from the surface to the antenna. Second, results indicate that the normalized second moment value relatively increases as the frequency of the source is decreased. An investigation of the characteristics of the antenna used in this project was made in an attempt to explain

this phenomenon. Analysis of the antennas near and far-fields was conducted (Appendix F). Results of this analysis indicate no apparent influence of recorded data based on the antennas near and far-fields. Therefore, the following hypothesis is introduced in order to explain the recorded data:

The data that was recorded in this project consisted of a 17 dB horn at X-band and a 25 dB horn at K-band. Since the 17 dB horn results in a larger illumination of the surface relative to the surface illumination of the 25 dB horn, more scattering will occur which results in higher 2nd moment values at X-band. However, it should be also noted that an averaging effect occurs resulting in higher first moment when the same antenna is used for transmit and receive. But the data implies that the increase in scattering is much more dominant than the averaging effect.

Finally, it was determined that the returned field intensity also has log-normal distribution. However, no evidence supports the conjecture that the field intensity distribution must match the distribution of the surface.

#### Recommendations

It is recommended that further investigations into electromagnetic wave scattering from rough surfaces be concentrated into the following areas:

1. antennas characteristics - to determine the validity of the hypothesis stated in the conclusion
2. higher and lower frequency analysis - to determine the limit influences of very rough

and very smooth surfaces

3. different surfaces analysis - to determine the electromagnetic scatter characteristics of different distributed surfaces
4. determination of a quantitative expression for the returned scatter based on surface statistics



## APPENDIX A

### LOG-NORMAL DISTRIBUTION

A random variable  $X$  is said to have a log-normal distribution if its logarithm ( $\ln X$ ) is normally distributed with parameters  $\mu$  and  $\sigma$ .

Suppose that variate  $Y$  is normally distributed with parameters  $\mu$  and  $\sigma$ . Now, if a new random variable is defined by  $X = e^Y$ , then the distribution function of  $X$  is

$$\begin{aligned} F_X(t) &= P\{X \leq t\} = P\{e^Y \leq t\} = P\{Y \leq \ln t\} \\ &= (2\pi)^{-1/2} \int_{-\infty}^{(\ln t - \mu)/\sigma} e^{-z^2/2} dz \end{aligned} \quad (11)$$

Hence, the density function of  $X$  is

$$\begin{aligned} f_X(t) &= \frac{(2\pi)^{-1/2}}{\sigma} t^{-1} \exp\left[-\frac{1}{2\sigma^2}(\ln t - \mu)^2\right] \quad t > 0 \quad \sigma > 0 \\ &= 0 \text{ elsewhere} \end{aligned} \quad (12)$$

which is the density function of the log-normal distribution.

The  $k$ th moment of  $X$  is

$$E(X^k) = \frac{(2\pi)^{-1/2}}{\sigma} \int_{-\infty}^{\infty} t^{k-1} \exp\left[-\frac{1}{2\sigma^2}(\ln t - \mu)^2\right] dt \quad (13)$$

and upon letting  $\ln t = z$ ,

$$E(x^k) = \frac{(2\pi)^{-1/2}}{\sigma} \int_{-\infty}^{\infty} e^{zk} \exp\left[-\frac{1}{2\sigma^2}(z - \mu)^2\right] dz$$

$$\begin{aligned}
&= \frac{(2\pi)^{-1/2}}{\sigma} \exp[k\mu + (k^2\sigma^2/2)] \int_{-\infty}^{\infty} \exp[-1/2(\frac{z-\mu}{\sigma} - k\sigma)^2] dz \\
&= \exp(k\mu + \frac{k^2\sigma^2}{2})
\end{aligned} \tag{14}$$

By letting  $k = 1$ , the first moment is found to be

$$E[x] = \exp(\mu + \frac{\sigma^2}{2}) \tag{15}$$

and by letting  $k = 2$ , the second moment is

$$E[x^2] = \exp(2\mu + 2\sigma^2) \tag{16}$$

The normalized second moment  $N_2$  of the log-normal distribution becomes

$$N_2 \triangleq \frac{E[x^2]}{\{E[x]\}^2} = \exp(\sigma^2) \tag{17}$$

It is of prime interest to express the normalized  $k$ th moment  $N_k$  as a function of  $N_2$ . Therefore

$$N_k \triangleq \frac{E[x^k]}{\{E[x]\}^k} = \frac{\exp(k\mu + k^2\sigma^2/2)}{\exp(k\mu + \frac{k\sigma^2}{2})} \tag{18}$$

which yields

$$N_k = \exp[\frac{\sigma^2}{2} k(k-1)] = [\exp(\sigma^2)]^{\frac{k}{2}(k-1)} \tag{19}$$

since  $\exp(\sigma^2) = N_2$

The normalized  $k$ th moment is found to be

$$N_k = N_2^{\frac{k}{2}(k-1)} \tag{20}$$

From the above equations, solving for the mean value  $\mu$  and the variance  $\sigma^2$  corresponding to the normal distribution Y yield:

$$\sigma^2 = \ln N_2 \quad \text{and} \quad (21)$$

$$\mu = \ln \left\{ \frac{E[x]}{N_2^{1/2}} \right\} \quad (22)$$

where  $E[x]$  and  $N_2$  are respectively the mean and the normalized second moment of the log-normal distribution  $f_X(t)$ .

APPENDIX B

PROGRAM TO COMPUTE THE MOMENTS OF THE SURFACE  
AND THE AUTOCORRELATION FUNCTION

TODAY'S DATE: 09-MAY-80  
CURRENT TIME: 14:21:00

READY  
OLD DY1: ELIIN

READY  
LIST

ELIIN 09-MAY-80 14:21:36

```
5 DISPLAY CLEAR
10 DIM V(2000)
20 PRINT "ENTER THE NUMBER OF DATA POINTS ";
30 INPUT P
40 IF P>4999 GO TO 20
50 OPEN "DY1:ELI" FOR OUTPUT AS FILE #1
60 FOR X=1 TO P
70 PRINT "ENTER DATA POINT NUMBER: ";X
80 INPUT A
90 V(X-1)=A
100 PRINT #1,A
120 I1=A+I1
130 I2=A*A+I2
140 I3=A*A*A+I3
150 I4=A*A*A*A+I4
160 I5=A*A*A*A*A+I5
170 NEXT X
175 CLOSE #1
180 I1=I1/P
190 I2=I2/P
200 I3=I3/P
210 I4=I4/P
220 I5=I5/P
230 N2=I2/I1/I1
240 N3=I3/I1/I1/I1
250 N4=I4/I1/I1/I1/I1
```

```
260 N5=I5/I1/I1/I1/I1/I1
270 PRINT "I1          I2          I3          I4          I5"
280 PRINT I1,I2,I3,I4,I5
290 PRINT "N2          N3          N4          N5"
300 PRINT N2,N3,N4,N5
310 OPEN "SY1:COR.DAT" FOR OUTPUT AS FILE #1
320 FOR B=0 TO (P-1)/2
330 A=0
340 FOR K=0 TO (P-B-1)
350 A=V(K)*V(K+B)+A
360 NEXT K
370 F=A/(P-B)
380 PRINT #1,F
390 NEXT B
395 CLOSE #1
400 COMMON P
410 CHAIN "DY1:COROUT"
```

APPENDIX C

PROGRAM TO PRINT AND PLOT THE CORRELATION OUTPUT

READY  
LIST

COROUT 13-MAY-80 15:51:22

```
20 OPEN "DY1:COR" FOR INPUT AS FILE #1
25 RESTORE #1
27 I=0
30 FOR X=1 TO P/2
40 I=I+1
50 INPUT #1,F
60 PRINT F
80 IF I=20 THEN PRINT "ENTER RETURN KEY TO CONTINUE.":I=0:INPUT D$ Δ
100 NEXT X
110 CLOSE #1
120 PRINT "DO YOU WANT TO COLLECT MORE DATA Y/N"
130 INPUT D$
140 IF D$="Y" THEN CHAIN "DY1:COMOIN"
142 OPEN "SY1:COR" FOR INPUT AS FILE #1
145 DIM A(201),Z(201)
150 FOR X=0 TO (P-1)/2
160 INPUT #1,A(X)
165 Z(X)=X
170 NEXT X
180 PRINT "ENTER THE NUMBER OF DATA POINTS YOU WANT PLOTTED<200";
190 INPUT J1
200 IF J1>200 GO TO 180
210 GRAPH(,J1,2(0),A(0))
220 PRINT "DO YOU WANT TO SEE ANOTHER GRAPH";
230 INPUT A$
235 DISPLAY CLEAR
240 IF A$="Y" THEN GO TO 180
250 PRINT "DO YOU WANT TO SEE THE DATA POINTS AGAIN";
260 INPUT A$
270 IF A$="Y" THEN GO TO 25
280 CLOSE #1
290 END
```

Δ :Is the delimiter used for multiple statement lines

APPENDIX D

PROGRAM TO COMPUTE THE MOMENTS OF THE FIELD  
INTENSITY UTILIZING THE A/D CONVERTER

READY  
OLD DY1: COMOIN

READY  
LIST

COMOIN 09-MAY-80 14:43:33

```

5 DISPLAY CLEAR
10 DIM V%(4999)
20 PRINT "ENTER THE NUMBER OF DATA POINTS ";
30 INPUT P
40 IF P>4999 GO TO 20
50 PRINT "ENTER THE SAMPLE RATE IN HERTZ ";
60 INPUT R
70 R1=1/R
80 AIN(("FAST",V%( ),P,R1,0,1)
90 PRINT "SAMPLING IS DONE."
100 FOR X=0 TO (P-1)
110 A=V%(X)*5.11743/2047
120 I1=A+I1
130 I2=A*A+I2
140 I3=A*A*A+I3
150 I4=A*A*A*A+I4
160 I5=A*A*A*A*A+I5
170 NEXT X
180 I1=I1/P
190 I2=I2/P
200 I3=I3/P
210 I4=I4/P
220 I5=I5/P
230 N2=I2/I1/I1
240 N3=I3/I1/I1/I1
250 N4=I4/I1/I1/I1/I1
260 N5=I5/I1/I1/I1/I1/I1
270 PRINT "I1          I2          I3          I4          I5"
280 PRINT I1,I2,I3,I4,I5

```

```
290 PRINT "N2          N3          N4          N5"
300 PRINT N2,N3,N4,N5
310 OPEN "SY1:COR.DAT" FOR OUTPUT AS FILE #1
320 FOR B=0 TO (P-1)
330 A=0
340 FOR K=0 TO (P-B-1)
350 A=V%(K)*5.11743/2047*V%(K+B)*5.11743/2047+A
360 NEXT K
370 F=A/(P-B)
380 PRINT #1,F
390 NEXT B
395 CLOSE #1
400 COMMON P
410 CHAIN "DY1:COROUT"
```



## APPENDIX E

## MEANS AND MOMENTS PROGRAM FOR TI/59

000	76	LBL	041	54	)	082	99	PRT	123	32	X:T
001	11	A	042	99	PRT	083	92	RTN	124	65	x
002	98	ADV	043	92	RTN	084	53	(	125	43	RCL
003	79	$\bar{x}$	044	76	LBL	085	43	RCL	126	07	07
004	32	X:T	045	15	E	086	07	07	127	55	÷
005	99	PRT	046	53	(	087	55	÷	128	43	RCL
006	92	RTN	047	53	(	088	43	RCL	129	03	03
007	76	LBL	048	43	RCL	089	03	03	130	85	+
008	12	B	049	21	21	090	75	-	131	06	6
009	53	(	050	65	x	091	03	3	132	65	x
010	43	RCL	051	33	X <sup>2</sup>	092	65	x	133	79	$\bar{x}$
011	11	11	052	54	)	093	79	$\bar{x}$	134	32	X:T
012	22	INV	053	34	FX	094	32	X:T	135	33	X <sup>2</sup>
013	45	Y <sup>x</sup>	054	54	)	095	65	x	136	65	x
014	43	RCL	055	53	(	096	43	RCL	137	43	RCL
015	03	03	056	35	1/X	097	05	05	138	05	05
016	54	)	057	65	x	098	55	÷	139	55	÷
017	99	PRT	058	43	RCL	099	43	RCL	140	43	RCL
018	92	RTN	059	20	20	100	03	03	141	03	03
019	76	LBL	060	54	)	101	85	+	142	75	-
020	13	C	061	99	PRT	102	79	$\bar{x}$	143	03	3
021	53	(	062	92	RTN	103	32	X:T	144	65	x
022	43	RCL	063	76	LBL	104	65	x	145	79	$\bar{x}$
023	03	03	064	16	A <sup>r</sup>	105	33	X <sup>2</sup>	146	32	X:T
024	55	÷	065	98	ADV	106	65	x	147	33	X <sup>2</sup>
025	43	RCL	066	53	(	107	02	2	148	33	X <sup>2</sup>
026	17	17	067	79	$\bar{x}$	108	54	)	149	54	)
027	54	)	068	32	X:T	109	42	STO	150	42	STO
028	99	PRT	069	33	X <sup>2</sup>	110	20	20	151	19	19
029	92	RTN	070	94	+/-	111	99	PRT	152	99	PRT
030	76	LBL	071	85	+	112	92	RTN	153	92	RTN
031	14	D	072	53	(	113	53	(	154	00	0
032	98	ADV	073	43	RCL	114	43	RCL	155	00	0
033	53	(	074	05	05	115	08	08	156	00	0
034	43	RCL	075	55	÷	116	55	÷	157	00	0
035	21	21	076	43	RCL	117	43	RCL	158	00	0
036	33	X <sup>2</sup>	077	03	03	118	03	03	159	00	0
037	35	1/X	078	54	)	119	75	-	160	00	0
038	65	x	079	54	)	120	04	4	161	00	0
039	43	RCL	080	42	STO	121	65	x	162	00	0
040	19	19	081	21	21	122	79	$\bar{x}$	163	00	0

## APPENDIX F

### NEAR-FIELD FAR-FIELD ANALYSIS

In order to determine the minimum distance between the transmitting antenna and the illuminated surface to be considered in the far-field (Fraunhofer zone), the phase difference between the center and the edge of the illuminated surface under test should be no greater than  $\frac{\lambda}{16}$  (Jasik, 1961).

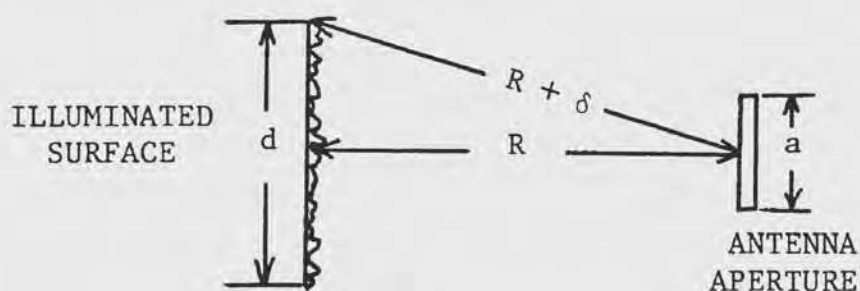


Fig. 14. Phase difference between center and edge of illuminated surface

Therefore, the minimum range distance  $R_{\min}$  is given by:

$$R_{\min} = 2 \frac{d^2}{\lambda} \quad (23)$$

Since aperture size and gain (G) are related by:

$$G = \frac{4\pi A_e}{\lambda^2} \quad (24)$$

where  $A_e$  is the effective aperture area, the dimension  $d$  may be obtained for simple aperture configuration.

For a circular aperture

$$R_{\min} = G \frac{2\lambda}{\pi} \quad (\text{ARRL, 1974}) \quad (25)$$

For the  $K_a$  band system;

$$G \approx 25 \text{ dB} \quad (\approx 316)$$

$$\lambda \approx 9 \text{ mm}$$

$$\text{Therefore, } R_{\min} = 316 \times 2 \times \frac{0.9}{\pi} = 57.63 \text{ cm} \quad \approx 58 \text{ cm}$$

For the X-band system

$$G \approx 17 \text{ dB} \quad (\approx 50)$$

$$\lambda \approx 3.33 \text{ cm}$$

$$\text{Therefore, } R_{\min} = 50 \times 2 \times \frac{3.33}{\pi} = 33.74 \text{ cm} \quad \approx 34 \text{ cm}$$

## BIBLIOGRAPHY

- American Radio Relay League. The ARRL Antenna Book. Newington: American Radio Relay League, 1974.
- Beckman, P., and Spizzichino, Andre'. The Scattering of Electromagnetic Waves from Rough Surfaces. New York: Macmillan, 1963.
- Cooper, George R., and McGillem, Clare D. Probabilistic Methods of Signal and System Analysis. New York: Holt, Rinehart & Winston, 1971.
- Davies, H. "The Reflection of Electromagnetic Waves from a Rough Surface." Proc. Inst. Electr. Eng. (London) 101 (1954): 211.
- Gibra, Isaac N. Probability and Statistical Inference for Scientists and Engineers. New Jersey: Prentice-Hall, 1973.
- Jasik, Henry. Antenna Engineering Handbook. New York: McGraw-Hill, 1961.
- Long, M. W. Radar Reflectivity of Land and Sea. Massachusetts: Library of Congress, 1975.